Comprehensive Heat Exchange Model for a Semiconductor Laser Diode

K. P. Pipe and R. J. Ram

***Abstract*—By measuring the total energy flow from an optical device, we can develop new design strategies for thermal stabilization. Here we present a comprehensive model for heat exchange between a semiconductor laser diode and its environment that includes the mechanisms of conduction, convection, and radiation. We perform quantitative measurements of these processes for several devices, deriving parameters such as a laser's heat transfer coefficient, and then demonstrate the feasibility of thermal probing for the nondestructive wafer-scale characterization of optical devices.**

***Index Terms*—Integrated optoelectronics, lasers, laser thermal factors, nondestructive testing, semiconductor device testing, semiconductor device thermal factors, semiconductor lasers, thermal variables measurement.**

I. Introduction

THERMAL MANAGEMENT is a critical issue in the performance of semiconductor laser diodes and other optoelectronic devices. Characteristic parameters such as device efficiency, stability, and lifetime are strongly dependent on operating temperature [1]–[3]. While internal heating and cooling sources such as recombination, Joule heating, and thermoelectricity have been studied extensively [4]–[6], external heat exchange models that describe the transport of energy to and from a device have focused primarily on the mechanism of thermal conduction [5]. Analysis of convective effects has been very limited [7].

Here, we present a comprehensive model for external energy exchange that examines other pathways such as convection and radiation. By taking into account all such mechanisms, we uncover design strategies for temperature control as well as arrive at a method for the wafer-scale testing of the light power of photonic integrated circuits that relies only on noninvasive thermal measurement.

II. External Heat Exchange

There are three mechanisms by which a device can exchange heat energy with its environment: conduction, convection, and radiation [8].

Conduction occurs across a temperature gradient through atomic vibrations and collisions in which no translational motion of the individual particles takes place; it is thus typical of solids. The heat equation that governs steady-state thermal conduction in a region with thermal conductivity k is given by $\nabla \cdot k\nabla T = -q$, where q is the power generated per unit volume. For quasi one-dimensional heat flow in a source-free region, the temperature difference ΔT between a boundary heat source and a point within the region can be approximated using a thermal impedance model as $\Delta T = Z_T Q_{\rm cond}$, where Z_T is a geometry-dependent impedance and $Q_{\rm cond}$ is the power generated by the source [5].

Convection occurs across a temperature gradient in which heat energy is transferred by the translational motion of individual particles; it is thus typical of fluids. The heat transferred by convection from a planar source surface of area A and temperature $T_{\rm surf}$ to a surrounding fluid at temperature $T_{\rm amb}$ is given by $Q_{\rm conv} = hA(T_{\rm surf} - T_{\rm amb})$, where the heat transfer coefficient h depends on parameters such as the fluid's velocity and specific heat and the nature of the fluid–surface contact.

Radiation occurs when carriers transmit electromagnetic waves; this energy can be acquired by the carriers thermally (as in blackbody radiation) or through electrical pumping (as in optoelectronic devices). For typical device temperatures, the blackbody term is small, but for optical devices such as laser diodes, the radiated power due to electrical pumping can be significant.

III. Heat Exchange Balance for a Laser Diode

In the steady state, the power generated by a device is balanced by the power removed from the device and we can write

$$Q_{\rm gen} = Q_{\rm cond} + Q_{\rm conv} + Q_{\rm rad}. \tag{1}$$

For a laser diode, we can write the radiated power below and above threshold as

$$Q_{\rm rad} = \begin{cases} \eta_{\rm LED} I, & (I < I_{\rm th}) \\ \eta_{\rm LED} I_{\rm th} + \eta_d (I - I_{\rm th}), & (I \geq I_{\rm th}) \end{cases} \tag{2}$$

where the external differential efficiencies $\eta_{\rm LED}$ and η_d are device-dependent and represent the fraction of recombining carriers that contribute to, respectively, spontaneous and stimulated emission.

For a semiconductor laser diode structure composed of a thin active region in contact with a thick substrate that also contacts a heat sink, we consider the typical case in which recombination and absorption are restricted to the vicinity of the active region and Joule heating in the substrate is small. Under these conditions, the bias power IV that is injected at the contacts is almost completely dissipated near the active region [9]. We can write the heat exchange balance for the laser diode, accounting

Manuscript received July 8, 2002; revised December 18, 2002. This work was supported by MIT Lincoln Laboratory and DARPA.

The authors are with Research Laboratory of Electronics, MIT, Cambridge, MA 02139 USA (e-mail: morgoth@mit.edu).

Digital Object Identifier 10.1109/LPT.2003.809308

for conduction through the substrate, convection from the top surface, and radiation from the active region as

$$IV = \frac{\Delta T}{Z_T} + A_{\text{eff}} h (T_{\text{surf}} - T_{\text{amb}}) + Q_{\text{rad}} \tag{3}$$

where $\Delta T = T_{\text{surf}} - T_{\text{hs}}$ is measured between the top surface electrical contact and the heat sink [10]. Due to lateral heat spreading, the area A_{eff} over which convection occurs is larger than the top contact area; however, we assume that it is small enough that air flow remains laminar and convection is proportional to $T_{\text{surf}} - T_{\text{amb}}$. Simple two-dimensional finite-element simulations that maintain constant heat sink and ambient temperatures confirm that total convected power remains proportional to surface temperature at different heat source magnitudes and, therefore, that A_{eff} does not vary with injected power in this approximation.

At zero bias ($I = 0$), convected and conducted power balance and (3) can be solved to give

$$A_{\text{eff}} h = \frac{\Delta T_0}{Z_T (T_{\text{amb}} - T_{\text{surf}})_0}. \tag{4}$$

Below threshold, assuming a low level of spontaneous emission, we can now write

$$Z_T IV = \Delta T - \Delta T_0 \frac{T_{\text{surf}} - T_{\text{amb}}}{(T_{\text{surf}} - T_{\text{amb}})_0} \tag{5}$$

and determine Z_T through thermal measurement below threshold.

IV. Experimental Determination of Heat Flow

To quantify heat exchange in actual devices, we examine two semiconductor laser diodes: a ridge-waveguide InP-based device that has a small top contact area and an oxide-stripe GaAs-based device that has a large contact area. We begin with the former, a 15×500 μm^2 five quantum-well InGaAsP–InP laser emitting at $\lambda = 1.55$ μm that sits atop a 100-μm-thick InP substrate that is mounted on a large ($4 \times 3 \times 0.4$ cm^3) gold-plated copper block heat sink. The copper block is cooled from below by an external Peltier cooler, and a thermistor located approximately 5 mm from the laser is used for heat-sink feedback control. To perform temperature measurements, we use 25×25 μm^2 NIST-traceable microthermocouples that have an accuracy of 200 mK and a resolution of 10 mK. Surface temperature T_{surf} is measured directly on the top surface contact and heat-sink temperature T_{hs} is measured on the heat sink approximately 50 μm from the substrate and just outside the light path. Surface temperature is measured at several locations and averaged; the variation across the surface is less than 200 mK.

Fig. 1 shows experimental data for this laser structure. We measure a series resistance of 0.9 Ω in the wires of the IV' power source and take this into account by setting $IV = IV' - I^2 R_{\text{series}}$. Although the thermistor is maintained at 17 °C, the large-area cooler is unable to effectively control the heat-sink temperature near the laser. In Fig. 1(b), we see that ΔT exhibits a kink at threshold due to the sudden increase in radiated power. By plotting the right side of (5) versus IV and fitting the slope below threshold, we determine Z_T to be 19.6 K/W. This value

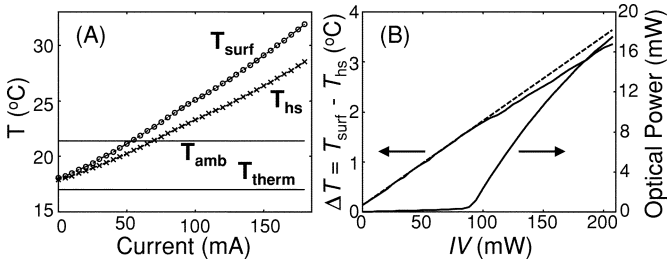

Fig. 1. (a) Measured temperatures of laser surface, heat sink, and ambient air. Thermistor set temperature is also shown. (b) Measured ΔT and direct optical power meter measurement.

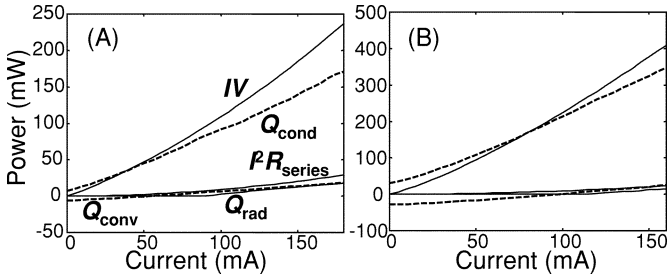

Fig. 2. Heat exchange terms as derived through thermal probing for devices at (a) $\lambda = 1.55$ μm and (b) $\lambda = 980$ nm. Conduction and convection terms are shown as dotted lines. Q_{rad} is measured using an optical power meter.

is close to previously reported values for geometrically similar InP-based laser diodes that were measured by different methods or predicted theoretically [9], [11], [12]. Small discrepancies may be due to thermal gradients in the heat sink [as shown in Fig. 1(a)] which lead to a nonisothermal boundary condition. Using (4), we measure $A_{\text{eff}} h$ to be 1.8×10^{-3} W/K. Although A_{eff} is unknown, an estimate that assumes one-dimensional heat flow ($Z_T \approx Z_T^{1D}, k = 68$ W/mK) yields $A_{\text{eff}} \approx 150 \times 500$ μm^2 and $h \approx 2.4 \times 10^4$ W/m^{2}K, the latter of which is comparable to reported experimental values for micron-scale semiconductor devices [13].

Having determined quantitatively the parameters for heat exchange, we can plot the contributions of the various mechanisms at different bias levels, as shown in Fig. 2. While conduction is the dominant term, the convected power is the same order of magnitude as the radiated power. Also shown are results for a 30×500 μm^2 oxide-stripe InGaP–InGaAs–GaAs device operating at $\lambda = 980$ nm that has a top contact size of 100×500 μm^2 and a GaAs substrate thickness of 100 μm. The same setup is used in both cases, and $R_{\text{series}} = 0.9$ Ω as before. For the GaAs device, we measure $Z_T = 16.3$ K/W and $A_{\text{eff}} h = 8.4 \times 10^{-3}$ W/K. The smaller Z_T and larger $A_{\text{eff}} h$ with respect to the InP device are most likely due to heat conduction into the large metal contact; the InP contact is only 15×500 μm^2 and is connected to a side contact pad. Estimating $Z_T \approx Z_T^{1D}$ as before, we find that $A_{\text{eff}} \approx 225 \times 500$ μm^2 and $h \approx 7.5 \times 10^4$ W/m^{2}K for the GaAs ($k = 55$ W/mK) device. The larger effective area is consistent with the larger contact size, and the greater heat transfer coefficient is most likely due to a more even temperature profile across the broad, high thermal conductivity contact, or possibly due to a greater surface roughness in the metal [8].

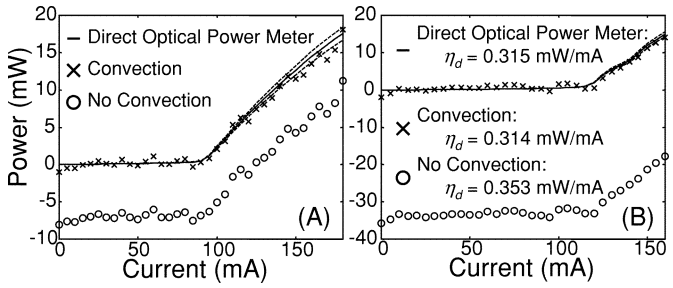

Fig. 3. Optical power as directly measured by a detector and as derived through thermal probing for devices at (a) $\lambda = 1.55$ μm and (b) $\lambda = 980$ nm. The elimination of convection from the thermal model causes the error in output power shown as well as a substantial error in Z_T.

In order to verify the accuracy of the experimental data, we plot $IV - Q_{\rm cond} - Q_{\rm conv}$ and compare it to measurements taken directly using an optical power meter. As shown in Fig. 3, the technique of thermal probing can be used to accurately measure the optical power output of the laser diodes. In Fig. 3(a), we model the InP laser both with and without convection included in the thermal model. In the zero-convection case, (5) becomes $Z_T IV = \Delta T$; the heat balance of (1) requires that heat conduction must rise accordingly, and Z_T is reduced to 17.1 K/W. Disregarding convection entirely, thus, results in an error for Z_T of 13%.

Since $A_{\rm eff}h$ is small for the InP laser, the zero-bias power convected into the device is likewise small ($\sim$ 6 mW), and $Q_{\rm conv}$ is approximately proportional to IV. For this reason, the convection and zero-convection models differ by only a constant 6 mW (although their values of Z_T are different). In the case of the GaAs laser, however, the zero-bias power convected into the device is larger ($\sim$ 29 mW) and a simple reduction in Z_T does not capture the bias dependence of the convection term. In Fig. 3(b), we model the GaAs laser with the convection term as well as with a zero-convection model. As before, the elimination of convection from the model reduces Z_T to 14.0 (an error of 14%), but now there is an additional bias-dependent error. This can be demonstrated by calculating the laser's differential efficiency above threshold η_d. By including the bias dependence of the convection term, the error in η_d is reduced from 12% to less than 1%. The differential quantum efficiency $\eta_d(q/h\nu)$ changes from 27.9% to the directly measured value of 24.8%. It is worth noting that the largest error reduction is at high bias values. For the InP laser, the error in η_d is 5%.

This technique shows promise as a means for the nondestructive wafer-scale testing of photonic integrated circuits for which detectors are unavailable or are unable to be placed in the light path, such as the case of a laser that is laterally coupled into a waveguide electro-absorption modulator [14]. A similar method has been proposed recently, which makes use of thermoreflectance microscopy of a laser's facet [15]. While this method utilizes the same general technique of relating device temperature to optical output, it is not applicable to wafer-scale testing. The advantage of the technique proposed here is that a simple setup may be used in a nondestructive way (that does not require calibration) on many different devices during normal operation.

V. Conclusion

By utilizing microthermocouple probes, we have experimentally quantified heat flow through the pathways of conduction, convection, and radiation in two optical devices, and have determined approximate values of the effective area and the heat transfer coefficient that are used in modeling convection heat exchange. Convection is often a nonnegligible effect and its absence in thermal models can result in errors in the measurement of thermal impedance of approximately 14%. The numerical models that are normally employed to predict parameters such as Z_T and T_0 for a packaged device can likewise suffer errors from the assumption of an isothermal heat-sink boundary condition, which we have shown to fail in certain common geometries.

By carefully accounting for all heat pathways, we have shown how this technique may be used for the nondestructive wafer-scale testing of optical devices. The location of lasing threshold is easily determined through temperature measurements, and light output power can be calculated to within a few percent. No prior knowledge of material parameters, geometry, or even light wavelength is necessary; all parameters are obtained experimentally. This method also shows promise for the determination of other laser parameters such as $\eta_{\rm LED}$ and for application to other devices such as optical amplifiers.

References

[1] H. J. Yi, J. Diaz, I. Eliashevich, M. Stanton, M. Erdtmann, X. He, L. J. Wang, and M. Razeghi, "Temperature dependence of threshold current density $J_{\rm th}$ and differential efficiency η_d of high-power InGaAsP/GaAs ($\lambda = 0.8$ μm) lasers," *Appl. Phys. Lett.*, vol. 66, p. 253, 1995.

[2] U. Menzel, A. Bärwolff, P. Enders, D. Ackermann, R. Puchert, and M. Voss, "Modeling the temperature dependence of threshold current, external differential efficiency and lasing wavelength in QW laser diodes," *Semiconductor Sci. Technol.*, vol. 10, p. 1382, 1995.

[3] H. K. Choi and G. W. Turner, "Mid-infrared semiconductor lasers based on antimonide compounds," in *Optoelectronic Properties of Semiconductors and Superlattices*, M. O. Manasreh, Ed. Amsterdam, The Netherlands: Gordon and Breach, 1997, vol. 3, p. 369.

[4] G. L. Tan, N. Bewtra, K. Lee, and J. M. Xu, "A two-dimensional nonisothermal finite element simulation of laser diodes," *IEEE J. Quantum Electron.*, vol. 29, pp. 822–835, Mar. 1993.

[5] L. A. Coldren and S. W. Corzine, *Diode Lasers and Photonic Integrated Circuits*. New York: Wiley, 1995, pp. 56–59.

[6] K. P. Pipe, R. J. Ram, and A. Shakouri, "Internal cooling in a semiconductor laser diode," *IEEE Photon. Technol. Lett.*, vol. 14, pp. 453–455, Apr. 2002.

[7] H. J. Lee, J. S. Yoon, and C.-J. Kim, "Numerical analysis on the cooling of a laser diode package with a thermoelectic cooler," *Heat Transf., Asian Res.*, vol. 30, p. 357, 2001.

[8] A. F. Mills, *Heat and Mass Transfer*. Boston, MA: Irwin, 1995.

[9] W. B. Joyce and R. W. Dixon, "Thermal resistance of heterostructure lasers," *J. Appl. Phys.*, vol. 46, p. 855, 1975.

[10] K. P. Pipe and R. J. Ram, "Experimental determination of heat flow in semiconductor lasers," in *Proc. Conf. Lasers and Electro-Optics*, Long Beach, CA, May 2002.

[11] W. Both and J. Piprek, "Thermal resistance of InGaAs/InP laser diodes," *J. Thermal Anal.*, vol. 36, p. 1441, 1990.

[12] J. S. Manning, "Thermal impedance of diode lasers: Comparison of experimental methods and a theoretical model," *J. Appl. Phys.*, vol. 52, p. 3179, 1981.

[13] N. Chong, T. A. S. Srinivas, and H. Ahmed, "Performance of GaAs microbridge thermocouple infrared detectors," *J. Microelectromech. Syst.*, vol. 6, p. 136, 1997.

[14] K. P. Pipe and R. J. Ram, "Method and apparatus for characterization of devices and circuits," U.S. Patent Pending, MIT Case 9501.

[15] S. Dilhaire *et al.*, "Laser diode light efficiency determination by thermoreflectance microscopy," *Microelectron. J.*, vol. 32, p. 899, 2001.